Adapting data survey analyses to beyond LambdaCDM cosmological models

Marie-Noëlle Célérier (LUX)

MNC PRD 110, 123526 (2024) arXiv: 2407.04452

Synergistic Power of Combined Cosmological Observables, 29 October 2025

Outline

1. Motivations and assumptions
2. The Szekeres solution
3. Constraints from standard cosmological observations
4. Effects present in inhomogeneous models only
5. Conclusion

Motivations and assumptions

(In)homogeneity of the Universe

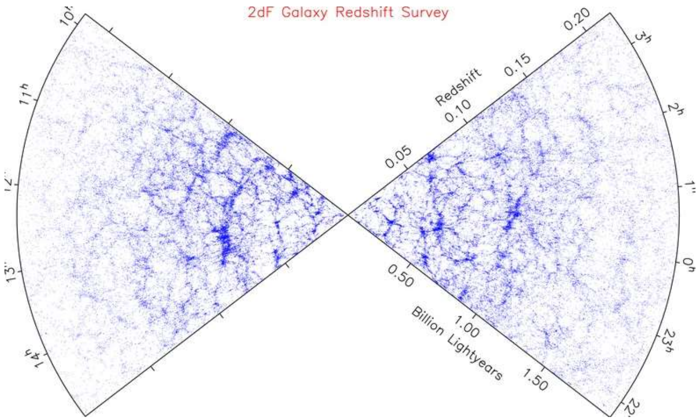

At large scales, the Universe is quasi-homogeneous.

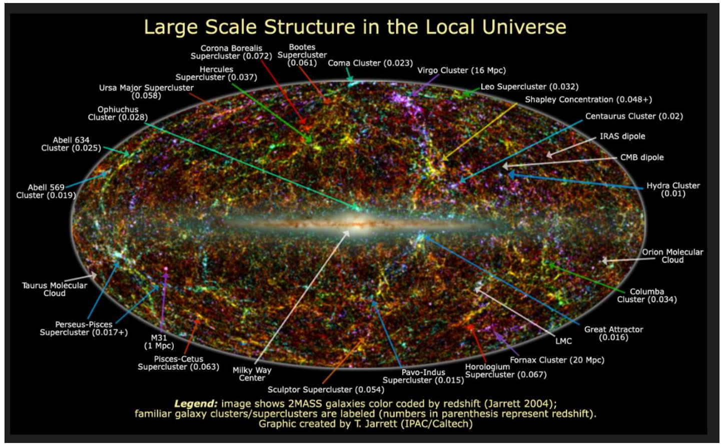

At small scales it is not.

LCDM tree (IAP INC group)

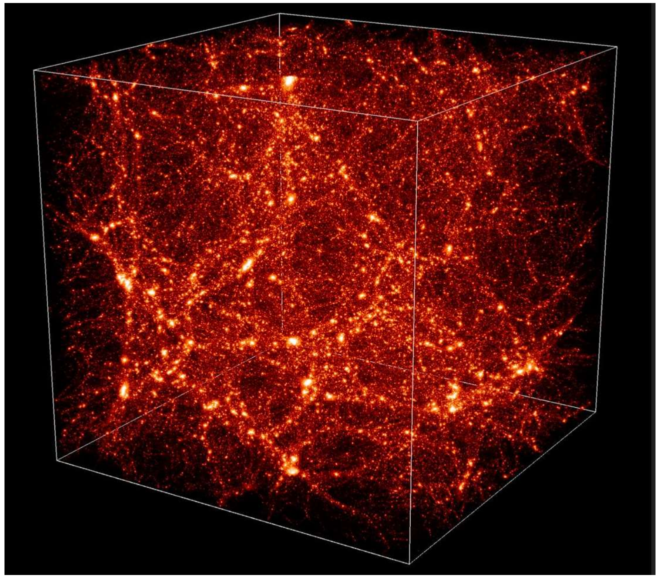

Marie-Noëlle Célérier , SPCCO workshop, 29 October 2025

Standard data analyses

Planck
Euclid
DES
DESI
Rubin
ACT
SPT
S4
…

analyses →

the ΛCDM parameters

$\Omega_b h^2 \quad \Omega_c h^2 \quad \theta_* \quad \tau \quad A_s \quad n_s$

or the commonly extended parameters

$H_0 \quad \Omega_\Lambda \quad \Omega_k \quad \Sigma m_\nu \quad N_{\rm eff} \quad w$

Cosmological tensions

essentially: H_0 and S_8 / σ_8

Mostly due to discrepancies between large scale measurements transported to the observer through an homogeneous standard model and local measurements realized in a lumpy region of the Universe

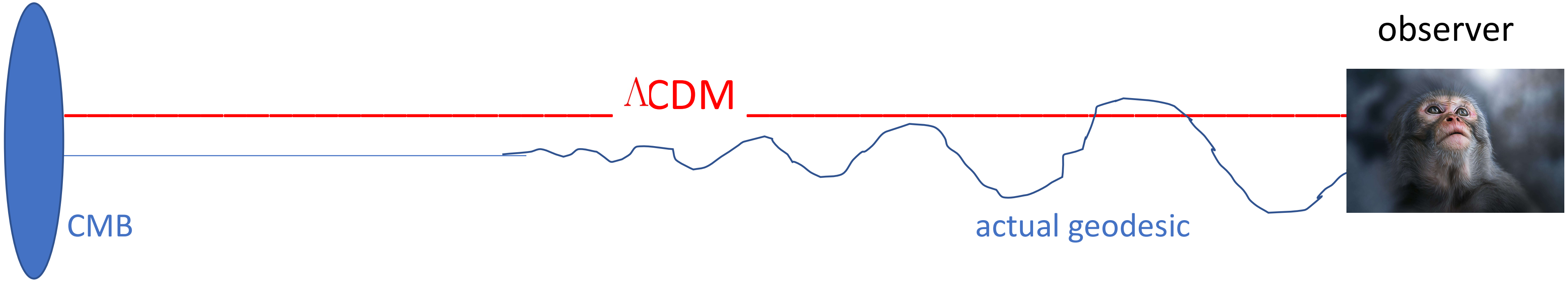

See: Di Valentino, Said, Riess +, The CosmoVerse White Paper: Addressing observational tensions in cosmology with systematics and fundamental physics, Phys. Dark Univ. 49 (2025) 101965, arXiv: 2504.01669

Anomalies

Large-scale anomalies in the CMB, examples:

- **hemispherical power asymmetry** (WMAP and Planck not sufficient to conclude, waiting for LiteBIRD, Gimeno-Amo + 2023)
- **lensing amplitude anomaly** (217 Ghz Planck data shows $A_{lens} > 1$ at 2.9σ, Addison + 2024)
- **cosmic dipole anomaly** (dipole measured from radio galaxy-quasar surveys > CMB kinetic dipole Secrest + 2025, Böhme + 2025)

Prefered expansion direction = symmetry axis (cosmography of Cosmicflows-3 and Pantheon Kalbouneh + 2023)

Inhomogeneity transition scale (largest superstructure reported to date: Quipu 428 Mpc Böhringer + 2025)

What if we merely consider the late time inhomogeneities without modifying anything else?

Assumptions

Gravitation theory: classical General Relativity

Geometric optics approximation:

Light wave-lengths are negligible wrt the space curvature scales:

- photons travel along null geodesics
- being test objects, the light rays have no effect on the geometry
- the light rays have no vorticity
- being geodesics, the light rays experience no acceleration

Reciprocity theorem:

Assumption: the photon number is conserved

Since we work in the framework of a metric theory of gravity (GR), the reciprocity theorem applies

Why keep GR as a gravitation theory?

TABLE I: Experimental Tests of General Relativity

#	Test / Observable	Experiment / Observation	Main GR Effect Tested	Precision / Deviation from GR	Reference / DOI
1	Weak Equivalence Principle (WEP)	MICROSCOPE satellite (CNES, 2017–2022)	Universality of free fall	$\Delta a/a < 1.3 \times 10^{-15}$	Touboul et al., PRL 129, 121102 (2022)
2	Local Position Invariance (Gravitational Redshift)	Gravity Probe A (NASA, 1976)	Frequency shift in gravitational potential	Verified to 7×10^{-5} (70 ppm)	Vessot et al., PRL 45, 2081 (1980)
3	Shapiro Time Delay (PPN γ)	Cassini spacecraft (2002–2003)	Time delay of radio signals near Sun	$\gamma = 1 + (2.1 \pm 2.3) \times 10^{-5}$	Bertotti et al., Nature 425, 374 (2003)
4	Light Deflection by the Sun	VLBI	Deflection of light by gravity	$\gamma = 1.00000 \pm 3 \times 10^{-5}$	Fomalont et al., ApJ 699, 1395 (2009)
5	Perihelion Advance of Mercury	Planetary ephemerides	Relativistic orbital precession	Agreement within $\sim 0.1\%$	Fienga et al., A&A 640, A118 (2020)
6	Geodetic & Frame-Dragging Precession	Gravity Probe B (NASA, 2011)	Geodetic & Lense–Thirring effects	Geodetic: 0.28%, Frame-dragging: 19%	Everitt et al., PRL 106, 221101 (2011)
7	Frame-Dragging in Satellite Orbits	LAGEOS & LARES (2013–2022)	Earth's rotation dragging spacetime	$\sim 2\%$	Ciufolini et al., Eur. Phys. J. C 82, 819 (2022)
8	Strong Equivalence Principle (Nordtvedt Effect)	Lunar Laser Ranging (LLR)	Universality of free fall for self-gravitating bodies	$\lvert\Delta a/a\rvert < 10^{-13}$	Murphy et al., Class. Quantum Grav. 38, 035013 (2021)
9	Binary Pulsar Orbital Decay	PSR B1913+16 (Hulse–Taylor)	Energy loss via gravitational waves	Agreement to 0.2%	Weisberg & Huang, ApJ 829, 55 (2016)
10	Double Pulsar Timing	PSR J0737–3039A/B	Multiple post-Keplerian parameters	Agreement within 10^{-4}	Kramer et al., PRX 11, 041050 (2021)
11	Gravitational Wave Speed & Polarization	LIGO–Virgo–KAGRA	Tensor nature & luminal speed of GWs	$\lvert v_{gw} - c\rvert/c < 10^{-15}$	Abbott et al., PRL 119, 161101 (2017)
12	Black Hole Shadow	Event Horizon Telescope (M87*, Sgr A*)	Light propagation near horizon	Consistent within $\sim 10\%$	Akiyama et al., ApJL 875, L1–L6; 930, L12 (2019, 2022)
13	Strong-Field GW Dynamics	LIGO–Virgo merger signals	Nonlinear dynamics, no-hair theorem	Deviations < 1%	Abbott et al., PRL 123, 011102 (2019)
14	Cosmological Tests (Lensing & Growth)	Planck, DES, Euclid (forecast)	Metric perturbations, gravitational slip	$\lvert\gamma_{PPN} - 1\rvert < 10^{-3}$	Planck Collab., A&A 641, A6 (2020)
15	Quantum Tests of WEP	Cold Atom Interferometry	Quantum universality of free fall	Verified to 10^{-12}–10^{-13}	Asenbaum et al., PRL 125, 191101 (2020)

Tests successfully passed and deviations severely bounded (precision down to 7.6×10^{-21} , JILA Millimiter-Scale Time Dilation)

The Szekeres solution

Szekeres metric

Exact solution of GR for an irrotational dust sourced spacetime with no symmetry = matter dominated region of the Universe. In comoving and synchronous coordinates:

$$\mathrm{d}s^2 = -\mathrm{d}t^2 + \frac{\left(\Phi_{,r} - \Phi E_{,r}/E\right)^2}{\epsilon - k}\mathrm{d}r^2 + \frac{\Phi^2}{E^2}(\mathrm{d}p^2 + \mathrm{d}q^2)$$

$$\Phi(t,r) \qquad\qquad k(r)$$

$$E(r,p,q) = \frac{S}{2}\left[\left(\frac{p-P}{S}\right)^2 + \left(\frac{q-Q}{S}\right)^2 + \epsilon\right]$$

$$S(r), \quad P(r), \quad Q(r)$$

Szekeres geometry and mass dipoles

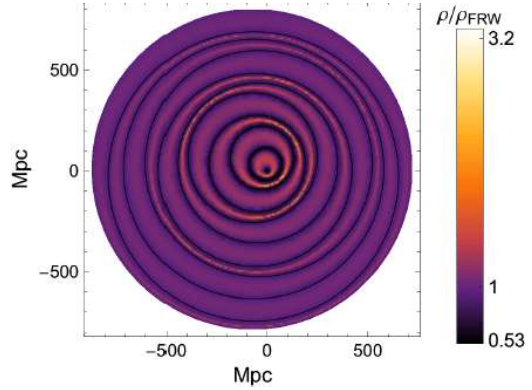

credit Buckley and Schlegel

- Quasi-spherical solutions $(\epsilon = +1)$= a set of non-concentric evolving spheres, with a dipole distribution of the energy density around each sphere

- Quasi-hyperbolic solutions $(\epsilon = -1)$ = a set of evolving hyperboloids, with a pseudo-spherical dipole

The strenght and orientation on each comoving slice in both classes are determined by $S(r), P(r), Q(r)$

- Quasi-planar solutions $(\epsilon = 0)$ have no dipole-like structure

A given Szekeres spacetime can have simultaneously quasi-spherical, quasi-hyperbolic and quasi–planar regions

Einstein's equations with a cosmological constant

1) $$\Phi_{,t}^2 = \frac{2M(r)}{\Phi} - k + \frac{\Lambda}{3}\Phi^2$$ integrated as $$t - t_B(r) = \int_0^{\Phi} \frac{\mathrm{d}\tilde{\Phi}}{\sqrt{\frac{2M}{\tilde{\Phi}} - k + \frac{\Lambda}{3}\tilde{\Phi}^2}}$$

Friedmann

$$\Downarrow$$

$$\dot{a}^2 = 8\pi G\rho a^2 - k + \frac{\Lambda}{3}a^2$$

Analogy: $$\Phi(t,r) \leftrightarrow a(t)$$

2) $$4\pi\rho(t,r,p,q) = \frac{M_{,r} - 3\grave{M}E_{,r}/E}{\Phi^2(\Phi_{,r} - \Phi E_{,r}/E)}$$

Szekeres parameters

Model a priori determined by 6 functions of r: $k(r)$, $S(r)$, $P(r)$, $Q(r)$, $M(r)$, $t_B(r)$, one quasi-constant parameter ϵ, and a cosmological constant Λ .

The number of independent functions can be reduced to 5 by rescaling r through, e. g., a choice of any arbitrary function.

Essential property of the Szekeres solutions: they possess the FLRW model as a homogeneous limit:

$$S = 2\epsilon,\ P = Q = 0,\ \Phi = ra(t),\ k = k_0 r^2,$$

r freedom $\Longrightarrow$ e. g. $t_B = const. = 0$

Other parameters: . the homogeneity-inhomogeneity transition scale, $z_{trans} < z_{eq}$, depending on the desired accuracy.

. the observer's location

ΛCDM parameters = numbers $\neq$ Szekeres parameters = functions

Null geodesic equations

Cosmological data obtained through electromagnetic signals (GW will come later)

Need of the Szekeres null geodesic equations $\Longrightarrow$

$$\frac{\mathrm{d}^2t}{\mathrm{d}s^2} + \left(\frac{\Phi_{,tr} - \Phi_{,t}E_{,r}/E}{\epsilon - k}\right)(\Phi_{,r} - \Phi E_{,r}/E)\left(\frac{\mathrm{d}r}{\mathrm{d}s}\right)^2 + \frac{\Phi\Phi_{,t}}{E^2}\left[\left(\frac{\mathrm{d}p}{\mathrm{d}s}\right)^2 + \left(\frac{\mathrm{d}q}{\mathrm{d}s}\right)^2\right] = 0,$$

$$\frac{\mathrm{d}^2r}{\mathrm{d}s^2} + 2\left(\frac{\Phi_{,tr} - \Phi_{,t}E_{,r}/E}{\Phi_{,r} - \Phi E_{,r}/E}\right)\frac{\mathrm{d}t}{\mathrm{d}s}\frac{\mathrm{d}r}{\mathrm{d}s} + \left(\frac{\Phi_{,rr} - \Phi E_{,rr}/E}{\Phi_{,r} - \Phi E_{,r}/E} - \frac{E_{,r}}{E} + \frac{k_{,r}}{2(\epsilon - k)}\right)\left(\frac{\mathrm{d}r}{\mathrm{d}s}\right)^2 + 2\frac{\Phi}{E^2}\left(\frac{E_{,r}E_{,p} - EE_{,rp}}{\Phi_{,r} - \Phi E_{,r}/E}\right)\frac{\mathrm{d}r}{\mathrm{d}s}\frac{\mathrm{d}p}{\mathrm{d}s} + 2\frac{\Phi}{E^2}\left(\frac{E_{,r}E_{,q} - EE_{,rq}}{\Phi_{,r} - \Phi E_{,r}/E}\right)\frac{\mathrm{d}r}{\mathrm{d}s}\frac{\mathrm{d}q}{\mathrm{d}s}$$
$$- \frac{\Phi}{E^2}\left(\frac{\epsilon - k}{\Phi_{,r} - \Phi E_{,r}/E}\right)\left[\left(\frac{\mathrm{d}p}{\mathrm{d}s}\right)^2 + \left(\frac{\mathrm{d}q}{\mathrm{d}s}\right)^2\right] = 0,$$

$$\frac{\mathrm{d}^2p}{\mathrm{d}s^2} + 2\frac{\Phi_{,t}}{\Phi}\frac{\mathrm{d}t}{\mathrm{d}s}\frac{\mathrm{d}p}{\mathrm{d}s} - \frac{\Phi_{,r} - \Phi E_{,r}/E}{\Phi(\epsilon - k)}(E_{,r}E_{,p} - EE_{,rp})\left(\frac{\mathrm{d}r}{\mathrm{d}s}\right)^2 + 2\frac{\Phi_{,r} - \Phi E_{,r}/E}{\Phi}\frac{\mathrm{d}r}{\mathrm{d}s}\frac{\mathrm{d}p}{\mathrm{d}s} - 2\frac{E_{,q}}{E}\frac{\mathrm{d}p}{\mathrm{d}s}\frac{\mathrm{d}q}{\mathrm{d}s} + \frac{E_{,p}}{E}\left[-\left(\frac{\mathrm{d}p}{\mathrm{d}s}\right)^2 + \left(\frac{\mathrm{d}q}{\mathrm{d}s}\right)^2\right] = 0,$$

$$\frac{\mathrm{d}^2q}{\mathrm{d}s^2} + 2\frac{\Phi_{,t}}{\Phi}\frac{\mathrm{d}t}{\mathrm{d}s}\frac{\mathrm{d}q}{\mathrm{d}s} - \frac{\Phi_{,r} - \Phi E_{,r}/E}{\Phi(\epsilon - k)}(E_{,r}E_{,q} - EE_{,rq})\left(\frac{\mathrm{d}r}{\mathrm{d}s}\right)^2 + 2\frac{\Phi_{,r} - \Phi E_{,r}/E}{\Phi}\frac{\mathrm{d}r}{\mathrm{d}s}\frac{\mathrm{d}q}{\mathrm{d}s} - 2\frac{E_{,p}}{E}\frac{\mathrm{d}p}{\mathrm{d}s}\frac{\mathrm{d}q}{\mathrm{d}s} + \frac{E_{,q}}{E}\left[\left(\frac{\mathrm{d}p}{\mathrm{d}s}\right)^2 - \left(\frac{\mathrm{d}q}{\mathrm{d}s}\right)^2\right] = 0.$$

and their first integral: $$\left(\frac{\mathrm{d}t}{\mathrm{d}s}\right)^2 = \frac{(\Phi_{,r} - \Phi E_{,r}/E)^2}{\epsilon - k}\left(\frac{\mathrm{d}r}{\mathrm{d}s}\right)^2 + \frac{\Phi^2}{E^2}\left[\left(\frac{\mathrm{d}p}{\mathrm{d}s}\right)^2 + \left(\frac{\mathrm{d}q}{\mathrm{d}s}\right)^2\right].$$

Redshift

Adapt to Szekeres the method applied by Bondi (1947) to the Lemaître-Tolman-Bondi solution, and obtain

$$\frac{\mathrm{d}(\ln(1+z))}{\mathrm{d}s} = -\frac{1}{\frac{\mathrm{d}t}{\mathrm{d}s}} \left\{ \left[\frac{\Phi_{,tr}\Phi_{,r} + \Phi\Phi_{,t}(E_{,r}/E)^2 - (\Phi_{,t}\Phi_{,r} + \Phi\Phi_{,tr})(E_{,r}/E)}{\epsilon - k} \right] \left(\frac{\mathrm{d}r}{\mathrm{d}s}\right)^2 + \frac{\Phi\Phi_{,t}}{E^2} \left[\left(\frac{\mathrm{d}p}{\mathrm{d}s}\right)^2 + \left(\frac{\mathrm{d}q}{\mathrm{d}s}\right)^2 \right] \right\}$$

Solve the null geodesic equations as 4 first order differential equations in $k^\mu = dx^\mu/ds$ with the two field equations satisfied, then calculate the redshift solving the above.

Distance equations

Calculation of the area distance:

The rate of change of the observer area distance depends on the expansion rate of the light bundle as

$$\frac{\mathrm{d}(\ln D_A)}{\mathrm{d}\lambda} = \theta = k^{\alpha}_{;\alpha}$$

which can be integrated as

$$D_A = \frac{\Phi^2}{E^2}\left(\frac{\Phi_{,r} - \Phi E_{,r}/E}{\sqrt{\epsilon - k}}\right) \exp\left[\int_{s_o}^{s} (k^t_{,t} + k^r_{,r} + k^p_{,p} + k^q_{,q})\mathrm{d}\lambda\right]$$

with the k^{α} and their derivatives obtained from the null geodesics.

Once D_A is known, the reciprocity theorem gives the luminosity distance $D_L = (1+z)^2 D_A$

Simplification of the model

Observation: the matter distribution and expansion are axially symmetric in the same direction Rubart & Schwarz 2013, Colin + 2017, Rameez + 2018, Kalbouneh + 2023, Secret + 2025, Wagenveld + 2025, Böhme + 2025

Theoretical implication: chose an axially symmetric Szekeres model

$$\Downarrow$$

$$P(r) = Q(r) = 0$$

Which, with $t_B(r) = 0 \quad (r \quad \text{freedom}) \Rightarrow$ 3 arbitrary functions to fit to data

Constraints from standard cosmological observations

Supernova data (standard method)

Type Ia supernovae are used as standard candles. Their apparent bolometric magnitude reads

$$m = \mathscr{M} + 5 \log D_L(z; p_a)$$

The magnitude zero point $\mathscr{M}$ can be measured from the apparent magnitude and redshift of low-redshift SNIa used as local calibrators whose distance is evaluated through, e. g., Cepheid variables, TRGB or JAGB.

Another set of measurements at higher redshifts is used to constraint the parameters p_a of the Szekeres model, included in the expression for D_L previously obtained.

Galaxy number counts

The total Szekeres rest mass in a volume element defined as the proper volume on a constant time slice, evaluated on the null cone, is

$$\mathcal{M} = 4\pi\rho\frac{\Phi^2}{E^2}\left(\frac{\Phi_{,r} - \Phi E_{,r}/E}{\sqrt{\epsilon - k}}\right)\mathrm{d}r$$

Inserting the Szekeres expression for the energy density

=> $$4\pi mn\frac{\mathrm{d}z}{\mathrm{d}r} = \frac{M_{,r} - 3ME_{,r}/E}{E^2\sqrt{\epsilon - k}}$$

=> the average mass density in redshift space, $m(z)n(z)$. Given the redshift calculated above, the mass density in real space follows and can be compared to the measured data => constraints on the Szekeres parameters.

Cosmic microwave background: CMB multipoles

In standard analyses of CMB data, the multipoles are determined by computing the coefficients of the spherical harmonic expansion

$$a_{lm} = \int_0^{2\pi} \int_0^{\pi} \frac{\Delta T}{T} Y_{lm}(\theta, \phi) \sin\theta \mathrm{d}\theta \mathrm{d}\phi$$ the CMB dipole is $$D = \sqrt{\sum_{m=-1}^{1} |a_{1m}|^2}$$

In Szekeres, the distribution of mass over each single (quasi)sphere is a dipole-like structure superposed on a monopole. This intrinsic dipole reads

$$\kappa \Delta\rho = \frac{(\chi_{,r} - \chi E_{,r}/E)(6M\Phi_{,r} - 2\Phi M_{,r})}{\Phi^2(\Phi_{,r} - \Phi E_{,r}/E)(\chi\Phi_{,r} - \Phi\chi_{,r})} \qquad \chi = \frac{1 + P^2 + Q^2}{2S} + \frac{S}{2}$$

To compare it with the measured CMB dipole: subtract the kinetic dipole due to our motion wrt the CMB rest frame.

This has been measured by Secrest + 2021, 2022, 2025.

Drawback: the CMB power spectrum term $C_l = \langle |a_{lm}|^2 \rangle$ is averaged over all directions.

In an anisotropic Szekeres universe, the dependence on m must be taken into account. To be considered in data analyses.

CMB: Sunyaev-Zeldovich effects

SZ effect = added spectral distortion of the CMB through inverse Compton scattering of the CB photons by high-energy electrons in galaxy clusters.

- Thermal SZ: the electrons owe their high-energy to their temperature

The TSZE gives the cluster area distance in a cosmology-independent way through (Birkinshaw + 1991)

$$D_A = \frac{N_{RJ}^2}{N_X}\left(\frac{m_e c^2}{k_B T_{eo}}\right)^2 \frac{\Lambda_{eo}}{16\pi T_{CMB}^2 \sigma_T^2 (1+z)^3}$$

which can be used to compare the Szekeres D_A with its measured value given by the above rhs.

Baryon acoustic oscillations

BAO measurements => the angular BAO scale $\theta_{BAO}(z) = \frac{r_s}{(1+z)D_A(z)}$

with the sound horizon $r_s = \int_{z_d}^{\infty} c_s(1+z)\mathrm{d}z$ and the sound speed $c_s(z) = \frac{1}{\sqrt{3\left(1+\frac{3\rho_b(z)}{4\rho_\gamma(z)}\right)}}$

Standard assumption: the acoustic scale is conserved along its travel through the late universe => considered as a standard ruler.

The outcomes of typical galaxy surveys (e.g., DESI) are displayed under a couple of comoving distances: $D_M(z) = r_s/\Delta\theta$ and $D_H(z) = r_s/\Delta z$

Reciprocity theorem for the comoving distance: $D_M = (1+z)D_A$

r_s independent of z => a set of measurements of BAO scales at different redshifts yield constraints on the Szekeres parameters from the $(1+z)D_A(z)$ factor in the expression for $\theta_{BAO}(z)$

Weak lensing

The magnification matrix of lens theory reads $\mathcal{A} = \begin{pmatrix} 1-\kappa-\gamma_1 & -\gamma_2-\omega \\ -\gamma_2+\omega & 1-\kappa+\gamma_1 \end{pmatrix}$

where the complex lensing shear $\gamma = \gamma_1 + \imath\gamma_2$ describes the stretching of galaxy images, the convergence κ, a change in size and brightness, and the rotation ω, the twisting or skewing of the image. From geometric optics $\omega = 0$ => $\mathcal{A}$ symmetric.

The optical tidal matrix $\mathcal{T}$ written in terms of the Szekeres Ricci and Weyl curvatures, gives the evolution of $\mathcal{A}$ through $\ddot{\mathcal{D}} = \mathcal{T}\mathcal{D}$, with $\mathcal{D} = D_A^{FLRW}\mathcal{A}$

Weak lensing surveys yield: source galaxy redshifts, galaxy positions on the sky, reduced shear estimates. The reconstruction of $\mathcal{A}$ can be done from these data and compared to the theoretical Szekeres lensing quantities.

Redshift drift

Redshift drift = redshift increase (or decrease) measured by an observer looking at the same source at different instants. The source is measured on the observer's two different past light cones.

It occurs in any expanding universe.

But its magnitude depends on the geometry of the region travelled by the rays => constraints on the Szekeres parameters from its measurement.

Tiny amplitude: of the order $10^{-18}\ s^{-1}$

Proposal (Wucknitz + 2021): use strong-gravitational-lens time delays to complete the drift measurement; time delay change over months and years can be interpreted as differential redshifts between the images

Effects present in inhomogeneous models only

Differential cosmic expansion-Hubble flow anisotropies

Inhomogeneous cosmological models (LTB, Szekeres, etc.) exhibit differential cosmic expansion which is a function of time and space.

FLRW <-> Szekeres: $a(t) \leftrightarrow \Phi(t,r)$

The expansion rate is split into two components: a transverse expansion and a longitudinal expansion. In Szekeres: $H_\perp = \frac{\Phi_{,t}}{\Phi}$ $\quad H_\parallel = \frac{\Phi_{,tr} - \Phi_{,t}E_{,r}/E}{\Phi_{,r} - \Phi E_{,r}/E}$

The overall rate of change is given by the scalar expansion $\theta = 2H_\perp + H_\parallel$

A survey providing, for each galaxy, its angular position, luminosity distance and redshift can be used to compute the redshift dependence of the local expansion. Compared to the Szekeres expressions above, they can constrain the model.

Cosmography

Cosmography = Taylor expansion of the luminosity distance in powers of the redshift. At third order:

$$d_L = d_L^{(1)} z + d_L^{(2)} z^2 + d_L^{(3)} z^3 + \mathcal{O}(z^4)$$

Each $d_L^{(i)}$ can be expressed wrt effective observational parameters (eop): effective Hubble, deceleration, jerk, curvature… parameters.

The dependence on the observation direction is taken into account through a multipole decomposition of these parameters (Heinesen 2021).

Each multipole of each eop is given an expression involving the hydrodynamical parameters of the timelike congruence of the matter: the expansion scalar, the acceleration vector, the shear and vorticity tensors.

Szekeres being acceleration and vorticity-free, the multipole expressions simplify.
The multipoles of each eop are written with the Szekeres parameter functions => shear > expansion.

Hills, Heinesen in preparation: going to the snap eop (fourth order in the redshift)

Position drift

A Szekeres observer who measures the same light source at different instants observes a drift in the redshift, but also in the position of the source.

The second ray is emitted in and received from a different direction by the observer who sees the source slowly drifting across the sky.

This can be calculated by a method inspired from Krasinski and Bolejko 2011.

This effect occurs in other inhomogeneous cosmological model, e. g., non-radial rays in LTB.

The only spacetimes of the Szekeres family where the position drift vanishes are FLRW => an observation of this drift for any remote source = the Universe is inhomogeneous up to the probed scales.

Effect too tiny ($\sim 10^{-6} - 10^{-7} \mathrm{arcsec/year}$) to be measured soon 

But technical progress hope 

Physical constraints

Metric signature preservation: $\epsilon - k > 0$ (save where $\Phi_{,r} - \Phi E_{,r}/E = 0$) => different evolution type depending on the value of ϵ

Shell-crossings avoidance: SCs are loci where the energy density diverges => must be avoided. Conditions for SC avoidance have been worked out by Szekeres 1975 and Hellaby and Krasinski 2002,2008

Positive areal radius: $\Phi(t,r) > 0, \quad \forall t \quad \text{and} \quad r$

Metric non degenerate and nonsingular: => non-vanishing E and S

Weak energy condition: either $M_{,r} - 3ME_{,r}/E \geq 0 \quad \text{and} \quad \Phi_{,r} - \Phi E_{,r}/E \geq 0$ or $M_{,r} - 3ME_{,r}/E \leq 0 \quad \text{and} \quad \Phi_{,r} - \Phi E_{,r}/E \leq 0.$

Asymptotic recovery of an FLRW universe at large scales: => $S = 2\epsilon, \quad P = Q = 0, \quad \Phi(t,r) = rR(t), \quad k = k_0 r^2$ for $t \geq t_{trans}$ and $r \geq r_{trans}$

Fixation of the r coordinate freedom: multiple possible choices depending on the considered effects MNC 2024

All the free functions must be differentiable

Conclusion

Compared data analyses

ΛCDM constant parameters

$$\Omega_b h^2 \quad \Omega_c h^2 \quad \theta_* \quad \tau \quad A_s \quad n_s$$

Or the extended parameters

$$H_0 \quad \Omega_\Lambda \quad \Omega \quad \Sigma m_\nu \quad N_{\rm eff} \quad w$$

Standard data analyses

Szekeres 3 functions and 7 constant parameters

$$k(r) \quad M(r) \quad S(r) \quad \epsilon \quad \Lambda$$

$$z_{trans} \quad \{t_0, r_0, p_0, q_0\}$$

regression methods for the functions

consider anisotropy, e. g., the m index in CMB a_{lm}

Conclusion: modify accordingly the data analysis methods

Take-home messages

- We have currently reached the point where cosmological models such as ΛCDM can no more satisfy the requirements of precision cosmology
- Szekeres inhomogeneous models, including FLRW models as homogeneous limits, appear as a promising GR alternative, exact and as close to ΛCDM as needed to keep the most robust early predictions of the standard model
- They exhibit an intrinsic mass diplole which has been found in recent survey analyses
- Axial symmetry as exhibited in galaxy survey and cosmographical study of expansion can be used to simplify the model
- The three functions of the r coordinate and the seven constants defining the Szekeres universe model can be identified through current and in-coming data surveys
- An adaptation to Szekeres of the data reduction processes in all cosmological surveys is essential to avoid systematic bias

THANK YOU FOR YOUR ATTENTION

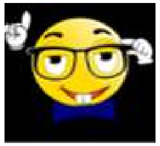

Pseudo-spherical dipole in quasi-hyperbolic solutions